Solid-State Electronics 225 (2025) 109078

Contents lists available at ScienceDirect

Solid State Electronics

journal homepage: www.elsevier.com/locate/sse

3D (micro/nano) CdO/p-Si co-doped Zn and La heterojunctions perform as solar light photodetectors

Bestoon Anwer Gozeh [a,b,*], Lary H. Slewa [c], Cheman Baker Ismael [d], Sarwar Ibrahim Saleh [d], Abdulkadir Yildiz [e], Fahrettin Yakuphanoglu [f]

[a] Department of Physics, College of Education/Shaqlawa, Salahaddin University-Erbil, Erbil, Kurdistan Region, Iraq
[b] Information Technology Department, Shaqlawa Technical College, Erbil Polytechnic University, Erbil, Kurdistan Region, Iraq
[c] Department of Physics, College of Science, Salahaddin University-Erbil, Erbil, Kurdistan Region, Iraq
[d] Radiology Department, Erbil Medical Technical Institute, Erbil Polytechnic University, Erbil, Kurdistan Region, Iraq
[e] Department of Physics, Faculty of Science and Arts, Kahramanmaraş Sü tçü Imam University, Kahramanmaraş, Turkey
[f] Nanoscience and Nanotechnology Laboratory, Firat University, Elazig, Turkey

ARTICLE INFO

Keywords:
Sol-gel method
Optical and electrical properties
Photodetector
Photoresponse

ABSTRACT

Cadmium oxide is among the most appealing materials since it may be utilized in a variety of applications, including photodetector. Al/La-Zn/co-doped CdO/p-type Si/Al photodetectors were fabricated using the sol–gel spin coat technique, with the CdO interface layer, varying concentrations of La (0.1, 0.5, 2, and 4 at%), and constant Zn (1 at%). Each film was grown on glass and silicon substrates so that their optical and electrical properties could be evaluated. Analyses were conducted on the morphological, optical, and electrical properties of transparent, co-doped CdO photodetectors. Using a field emission scanning electron microscope and energy dispersive X-ray, the morphological properties and elemental compositions of prepared materials The FESEM images revealed a 3-D micro/nanostructure of La/Zn-co-CdO form, characterized by the formation of microspheres by the use of nanoneedles. Additionally, the development rate of the films was observed to be inhibited by the co-doping of CdO with La-Zn. The transmittance measurements show that the prepared films exhibit a ranging from 40 to 70 % in the visible spectrum. The optical bandgap of prepared thin films measured by linear fitting where increases linearly with increasing La-Zn co-dopant concentration and was found in range between (2.07 and 2.27 eV). When CdO was co-doped with La (0.1 at%) and Zn (1 at%), the I-V properties of the produced photodetectors revealed high rectifying behavior. The photovoltaic and photoelectrical behaviors are shown, together with associated parameters. Additionally, the dopant concentration of (La 0.1 and Zn 1) at% has the highest photoresponse behavior at about 4085, surpassing findings in prior research. The highest photosensitivity of 6.3×10^{-4} has been determined for La 0.1 and Zn 1) at%. The strong rectifying characteristics, together with the photovoltaic, photoelectrical, and photoresponse properties, indicate that the fabricated (La 0.1 and Zn 1) at% co-doped CdO-based photodetector is suitable for optoelectronic applications, particularly in sensors and photodetectors.

1. Introduction

Photodetectors can be classified into various classes based on their working methods or device structures. These classes have been identified as photoconductive, PN junction photodiodes, phototransistor, and metal–semiconductor-metal (MSM) photodetectors. PN photodiodes are a type of photodetectors that utilize carrier generation in the high-field junction region. They exhibit significantly faster reaction times compared to photoconductors [1–4]. Transparent conducting oxide substances, including cadmium oxide (CdO), zinc oxide (ZnO), and tin oxide (SnO_2), are potential candidates for smart windows, light-emitting diodes (LED), heat reflectors, photovoltaics, solar cells, and gas sensor devices. CdO is a prominent material with great potential due to its direct and indirect band gaps of 2.24 eV and 0.89–0.99 eV, its mobility value of 216 $cm^2\ V^{-1}\ s^{-1}$, its low resistivity of $10^{-4}\ \Omega$ cm, and its high transparency to visible light [5]. It also exhibits n-type conductivity due to oxygen vacancies, and shallow donors contribute to the high charge concentration. Moreover, Si, which is widely used in the optoelectronics

* Corresponding author at: Department of Physics, College of Education/Shaqlawa, Salahaddin University-Erbil, Erbil, Kurdistan Region, Iraq
E-mail address: bestoon81@gmail.com (B.A. Gozeh).

https://doi.org/10.1016/j.sse.2025.109078
Received 18 September 2024; Received in revised form 20 January 2025; Accepted 25 January 2025
Available online 26 January 2025

industry and has a narrow band gap of 1.1 eV, is an appropriate material for IR and visible photodetection procedures [6]. Hence, to obtain a wide spectral photoresponse in photodetectors, the structure of CdO/Si is often utilized and is basically a good choice [5]. The transparent electrode within a self-contained p-n junction-equipped photodevice plays a critical role in achieving the necessary superior sensitivity and fast response times [7]. On the other hand, one of the most widely used structures for optoelectronic devices is a ZnO-based thin film due to its exceptional chemical, Optical, and electrical properties. ZnO provides several advantages for utilizing optoelectronic devices, such as significant exciton binding energy (60 meV), a large bandgap of 3.3 eV, non-toxicity, and high transparency. ZnO is a suitable material for a wide range of applications, such as photovoltaics, phototransistors, IR detectors, etc. [8]. Moreover, adding co-dopant elements has a great role in the research area due to changing material characteristics. La3+, which has a higher ionic radius of 0.116 nm compared to Cd2 + ions, but Zn2+, which has an ionic radius of 0.074 nm and a smaller radius, can easily replace Cd2+ (0.097) and penetrate into the CdO lattice. This inclusion behavior can be interesting and has played a critical role in scientific research. La-Zn/CdO could be obtained with different thin film deposition methods such as sputtering, spray pyrolysis, electrochemical techniques, atomic layer deposition, pulse laser deposition [9–14], etc. All of these techniques have their advantages and disadvantages, like high temperatures and pressures, which restrict the substrate types that could be used for coating. Moreover, the sol–gel technique provides perfect homogeneity, excellent control, and material combinations for coated materials, which could be beneficial for optoelectronic devices [15].

3D micro/nano-structures refer to 3D micro-sized particles composed of low-dimensional nanoparticles such as nanoflakes, nanorods, and nanoparticles. These structures possess the unique characteristics of nano-building blocks and can collectively benefit from the exceptional microscale secondary architectures. As a result, they can be used to create electrode materials with a large surface area and relatively strong structural stability. As a result of the literature, Jia et al. [16] examined the photovoltaic characteristics of La-doped ZnO nanowires and found that the La-doping concentration was very effective in increasing the efficiency of the photodevice. Yu Yun et al. [17] have reported a La-doped CdO thin film fabricated by molecular beam epitaxy and demonstrate that the La ion affected the optical characteristics of CdO. Lower resistivity and elevated concentrations of carriers for La-doped CdO were both reported by Velusamy et al. [18] as increasing the charge carrier concentration. Ortega et al. [19] have achieved from Zn-doped CdO heterojunction-based photodetectors, the thin layers on crystalline silicon demonstrate very good spectral response at both the blue and infrared regions of the visible light. It is highly desirable that the CdO-based photodetectors obtained by modifying the components with dopant elements have a good alternative to potential photodevice applications [20]. Furthermore, a lot of work is still required to fully understand the behavior of these promising photodetectors. In this study, La with various concentrations and Zn-CdO solutions have been produced by the sol–gel spin coating method to fabricate Al /p-Si/ La (0.1, 0.5, 2, and 4 at%)- Zn (1 at%) co-doped CdO/Al photodetectors. The target of this study is to develop low-cost but highly stable photodetectors with fast response durations and to improve the performance properties of thin film's photoresponse. Furthermore, the fabricated photodetectors were characterized to investigate the morphology, optical, and electrical properties using a scanning electron microscope, UV–vis spectrophotometer, and solar simulator device. The performance of the device is contingent upon voltage and frequency. The produced device exhibits significant sensitivity to solar light exposure, demonstrating a substantial photoresponse.

2. Experimental procedures

2.1. Photodetector Fabrications

For the preparation of the 3D (micro/nano) structure of La-Zn/co-doped CdO thin films at varying concentrations of La (0.1, 0.5, 2, 4 at %) and constant Zn (1 at%), 0.5 M of cadmium acetate dehydrates [CH3COO)2Cd·2H2O, MW = 266.53, extra-pure AR, 99 %] was used as the main source of CdO, and zinc acetate [(1 at%), Zn (CH3COO) 2·2H2O, MW = 219.49] along with lanthanum nitrate hexahydrate III [(0.1, 0.5, 2, and 4) at%, $La(NO_3)_3$, M_W = 433.01] were added as sources of dopant materials based on the results of [21,22]. In addition to adding ethanolamine [C_2H_7NO, M_W = 61.08, 0.3 ml] and 2-methyloxyethanol [$C_3H_8O_2$, M_W = 76.1 (10 ml)] to the prepared mixture, they were employed as stabilizers and solvents in the sol–gel procedure for the fabrication of thin films. The resulting mixture was magnetically stirred for three hours at 60 °C to generate a transparent and homogenous solution. The produced solutions were then aged in bottles for approximately 16 h. (111) surface orientation, 600 μm thickness, and resistance around 5–10 Ω.cm of single crystal p-type Si were used as substrates in the manufacture of photodetectors. At the beginning of the experiment, the silicon wafers had been cleaned. To remove the native oxide layer from the surface of the semiconductor, it was etched in hydrofluoric acid for about 30 s and then rinsed in an ultrasonic bath with double-deionized water for 2.5 min. Moreover, they were subsequently sterilized chemically by progressively immersing them in acetone and ethanol for two minutes each. After conducting the necessary cleansing procedures for the Si substrate, the ohmic back contact on the substrate was established utilizing Vaksis thermal evaporation technology. A thin layer of very pure Al metal was deposited onto the back of the silicon substrate, vaporizing it to the opaque side of the semiconductor at a rate of 10 A°/sec for 2 min under high vacuum conditions, an ohmic contact has been prepared on back side of Si wafer evaporating of Al metal (99.99 %) and thickness of 150 nm by thermal evaporation system at pressure of 4.5 10^{-5}Torr. In order to promote the establishment of ohmic contact between Al metal and Si substrate, annealing was conducted in a quartz tube furnace at 570 °C only for 5 min with nitrogen gas at a flow rate of 1 bar.

Furthermore, the La-Zn co-doped CdO samples generated via the sol–gel method were then coated by the spin coating technique on the other polished surface of the semiconductor at 3000 rpm for 30 sec, and thin films were produced. To get rid of organic residues, the films were immediately dried on a hot plate for five minutes at 250 °C based on previous work [23]. The technique was repeated until homogenous films with defined thickness were obtained, and the prepared samples were consequently annealed in a muffle furnace for one hour at 400 °C prior to making the front contact so that they might achieve a more durable structure.

The manufacturing process of Al/p-Si/La-Zn co-doped CdO/Al photodetectors was completed by depositing aluminum metal onto the surface of La-Zn/co-doped CdO layer, allowing current to flow vertically between the contacts. Aluminum metal was deposited onto the top layer via a mask with circulars electrode, each having a diameter of 1 mm, using the same thermal evaporation coating method and conditions used for creating the back contact. The round metallic rectifier contacts have an area of 7.85 10–3 cm2. Fig. 1 shows a schematic illustration of the manufactured electronic device.

2.2. Thin film characterization

The morphology and elemental composition of CdO thin film co-doped with various concentrations (0.1, 0.5, 2, 4 La, and Zn 1) at% were examined using field emission scanning electron microscopy (FESEM) Hitachi S-4800 at an accelerating voltage of 10 kV and a working distance of 4.9 mm. In addition, when combined with energy dispersive X-ray (EDX) spectroscopy, this device could also accurately

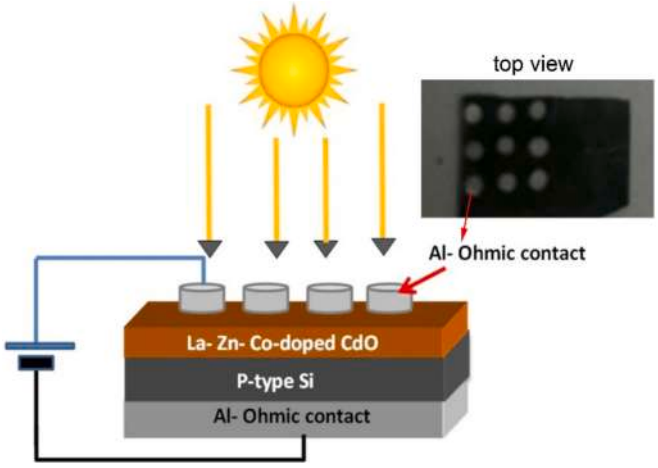

Fig. 1. Shows a schematic of the La and Zn co-doped CdO/ P-type Si heterojuction used as a photodetector.

ascertain the chemical composition of the thin films under identical conditions.

The optical properties of the prepared films were studied using a spin coater to apply La-Zn/co-doped CdO thin films with different concentrations of La (0.1, 0.5, 2, and 4 at%) and a constant Zn concentration (1 at%) on a glass substrate. Glass substrates, 2 mm thick, were cleaned in an ultrasonic bath with methanol and deionized water for 15 min, then dried with N2 gas. The spin coating process was conducted at a speed of 1600 rpm for 16 s, followed by drying at 250 °C for 11 min. Repeatedly following the procedure resulted in uniform films of a specified thickness. Furthermore, the films underwent annealing at a controlled temperature 400 °C for one hour in a muffle furnace. UV–VIS spectrometer (shimadzu-3600,) where used to study the optical properties of the thin film by measure the transmittance and absorbance spectrum at the range of 200 to 1000 nm wave length.

2.3. Photodetector characterization

The photodetectors capacitance–voltage (C-V) properties were measured using a computer-controlled Keithley 4200 semiconductor characterization device. Also, the characteristics of photoresponse, current–voltage (I-V), and current–time (I-t) characteristics were also measured automatically using the FYTRONIX FY 5000 photovoltaics system.

3. Result and discussion

3.1. The thickness measurement of thin films

The cadmium oxide thin films were doped with different concentrations of La and Zn (at 1 %) and applied to glass using the spin coating method described in the previous experimental section. La-Zn-co-doped CdO films clung strongly to the substrate and appeared homogeneous.

The thicknesses of the created film were determined using the gravimetric weight difference method, which is based on the glass pieces' stacked film weight divided by unit area (g/cm^2), and the thicknesses of film were calculated from the following equation:

$$T = \frac{1}{\rho}\frac{M}{A} \tag{1}$$

where T is film thickness, M is film mass in gram, A is film area in cm^2, and the film density is ρ [24]. The thickness of all coated films is approximately 560 nm.

3.2. Surface morphology and composition analysis

FE-SEM is used to examine the morphological alterations in CdO films co-doped with varying concentrations of La and Zn (1 at%). Fig. 2 displays various magnifications of FESEM images of La-Zn/co-doped CdO with varying La concentrations (0.1, 0.5, 2, and 4 at%) and a consistent Zn concentration (1 at%). All images display the 3D micro/nanostructure of La/Zn-co-CdO, consisting of microspheres formed by nanoneedles. At a lower concentration of La, the average diameter of the microsphere particle is 0.41 ± 0.14 μm and contains a nano-needle with an average diameter of 124 nm and a length of 22.7 nm. An increase in La doping concentration results in an increase in the size of the microsphere particle. At higher concentrations (Fig. 2d), the average diameter is 0.96 ± 0.17 μm, characterized by a uniform distribution of longer needles with a diameter of 21.32 nm. The surface microstructures of CdO films are significantly altered by changes in the concentrations of La in La/Zn co-doping CdO film, as evidenced by the analysis of FE-SEM images. Furthermore, the macroparticles evenly coat the surface of the silicon substrate without forming any aggregates.

The EDX technique was utilized to assess the elemental composition of La-Zn/co-doped CdO samples, which were synthesized with different La concentrations (0.1, 0.5, 2, and 4 at%) and a constant Zn content (1 at %). Fig. 3 displays the energy-dispersive X-ray (EDX) spectra of the CdO thin film sample, which has been co-doped with 0.1 (at%) of La and 1 (at %) of Zn. The table in Fig. 3 provides a comprehensive list of the identified components for all samples. The films comprised cadmium and oxygen constituents, in addition to zinc and lanthanum dopant. The atomic ratio of Cd/O in all samples is stoichiometric, with a value of 0.8. The value of Zn remains consistent, almost equal to 12 %, for various La concentrations (0.1, 0.5, 2, and 4 at%) with corresponding La % atomic values of 0.14, 0.48, 2.35, and 4.14.

3.3. Optical properties

The optical transmission spectrum of CdO thin films co-doped with varying concentrations of La (0.1, 0.5, 2, and 4 at%) and a constant Zn content (1 at%) in the wavelength range of 200–1000 is displayed in Fig. 4(a). The results indicated that transparent films absorb between 40 and 70 percent of the visible spectrum. With the exception of 2 at % of La. All the film samples demonstrate that the CdO films' transparency rises with constant Zn doping amounts of 1 at % and a variety of La dopants in the range between 300 and 650 nm. Since it is generally known that variations in transmittance rely on the material properties of the films, this change in transparency is connected to the structural qualities of the film characteristics. The change in the film's transparency demonstrates that the transmission at the smallest and greatest dopant levels attained the highest possible percentage of transparency. Numerous additional studies have reported the observation of similar random variations in transmittance when CdO is doped with La [15,18].

The transmission spectra of the films show an optical absorbance edge that corresponds to an abrupt decrease in the transparency of the thin film. Further, according to the equation [25], the Tauc's curve between a material's absorption coefficient (α) and the photon energy that is incident ($h\nu$) could be used to determine the coated material's optical bandgap (E_g), As presented in Fig. 4(b). The predicted bandgap values were shown in Fig. 4, calculated with a linear part extrapolation plot of $(\alpha\, h\nu)^2$ 2 vs. $h\nu$.

$$\alpha h\nu = B\left(h\nu - E_g\right)^n \tag{2}$$

$(\alpha = 2.3 Absorbance/t)$ is the Lambert–Beer law [26], where the absorption coefficient and thickness are defined by the terms (α) and (t), respectively, and (n = 1/2) for direct bandgap type. As seen in Fig. 4, the calculated bandgaps for the samples demonstrate that the measured value of Eg reduces from 2.2 to 2.08 eV. The sample with the greatest optical band gap, 2.23 eV, included 0.5 at% La dopant. The narrowing of

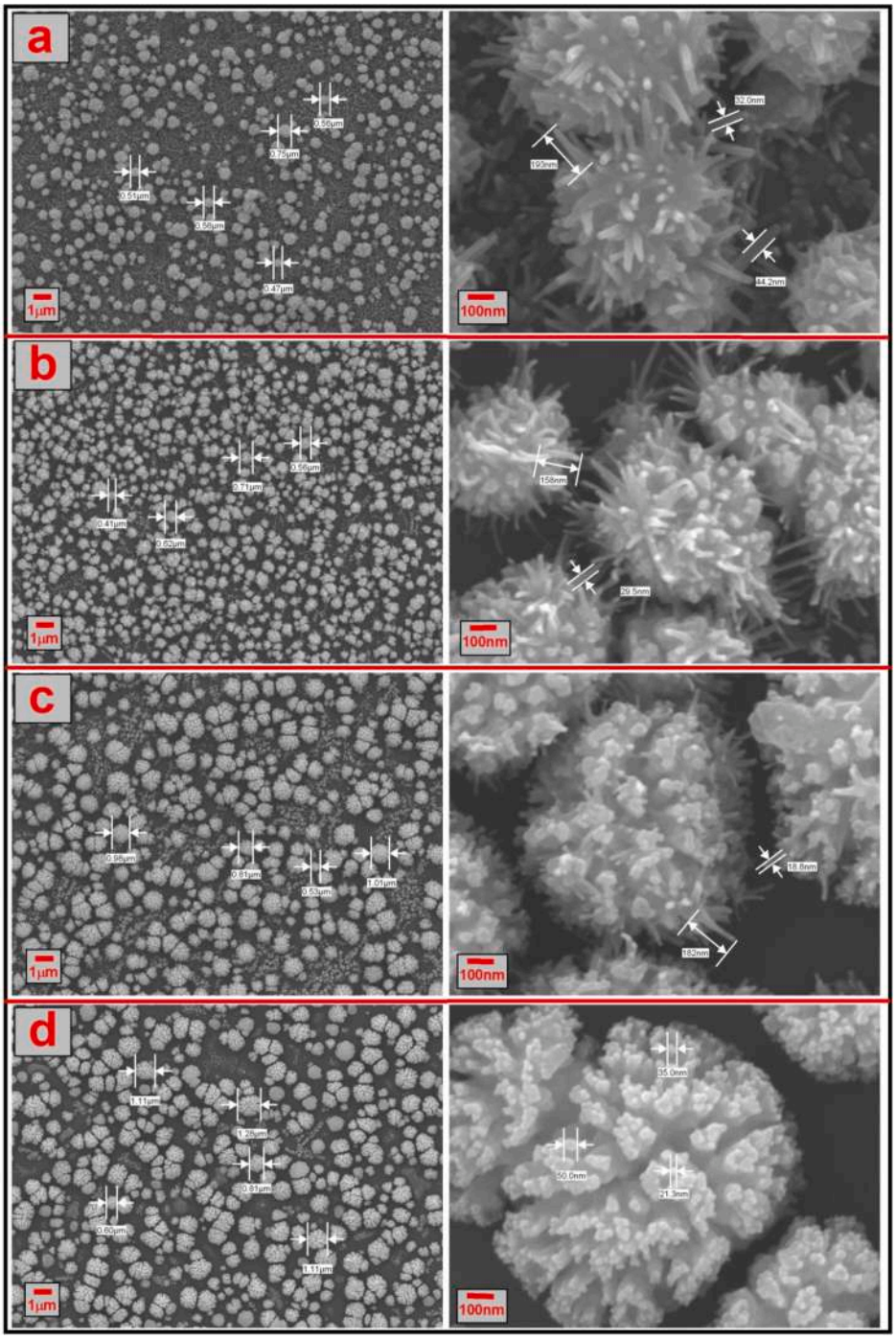

Fig. 2. The FESEM images at (a) 0.1, (b) 0.5, (c) 2, and (d) 4 of (La and Zn 1) at% co-doping CdO.

the bandgaps was likely caused by rare earth RE (La^{3+}) doping and was primarily brought on by two effects: RE ions introduce novel impurity bands and the robust Re-Oxygen orbital coupling [27]. Compared with [28] the bandgap was also evidence that narrowing with increasing La concentration, these changes can create mid gap states or cause a shift in the conduction band, which could lead to a decrease in the effective band gap.

3.4. Electrical properties and photoresponse

Studies on the I-V features of La-Zn co-doped CdO photodetectors were performed using solar light within 2 Volts and different illumination intensities. Fig. 5 shows the relation between I and V behaviours in the reverse and forward bias region that were taken under dark as well as in the presence of light, which are separated by large amounts of current. These intervals show that the rising illumination intensity of daylight in the photodetectors increases reverse current and the created object's sensitivity to light. In mentioned Fig. 5 show that the photodetector has a high rectifying behavior and has a rectification ratio of 1.28×10^5 at $\pm$ 3 V of (La 0.1 and Zn 1) at%, which is mainly attributed to the lower reverse current and higher forward current of the device. thus, the rectification ratio of the photodetector shows competitive advantages compared to other heterojunction photodetectors in previous literature [29–31].

In addition to the I-V characteristics, the Thermionic Emission Theory (TET) was utilized for calculating the parameters, like barrier height

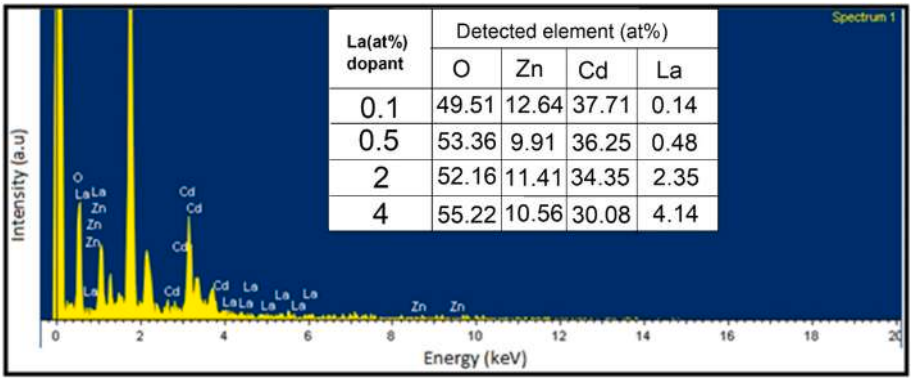

La(at%) dopant	Detected element (at%)			
	O	Zn	Cd	La
0.1	49.51	12.64	37.71	0.14
0.5	53.36	9.91	36.25	0.48
2	52.16	11.41	34.35	2.35
4	55.22	10.56	30.08	4.14

Fig. 3. EDX spectrum for a CdO thin film co-doped with La (0.1 at%) and Zn (1 at%) constant concentrations.

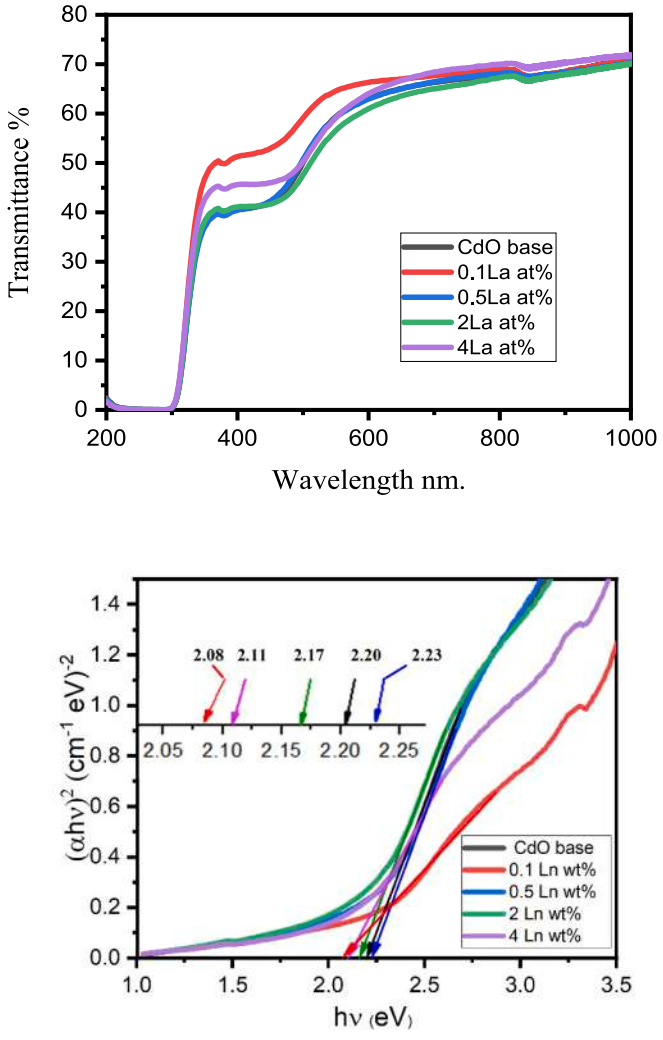

Fig. 4. (a) The optical transmission spectra, and (b) Tauc's plots of various (La and Zn1) at% co-doped CdO thin films.

as well as ideality factor, that are crucial parameters for the generated photodetector [32].

$$I = I_s \exp\left(\frac{q(V - IR_s)}{\eta kT}\right) - 1 \tag{3}$$

Thus, the I_s term in equation (3) shows the saturation current, as expressed as [23].

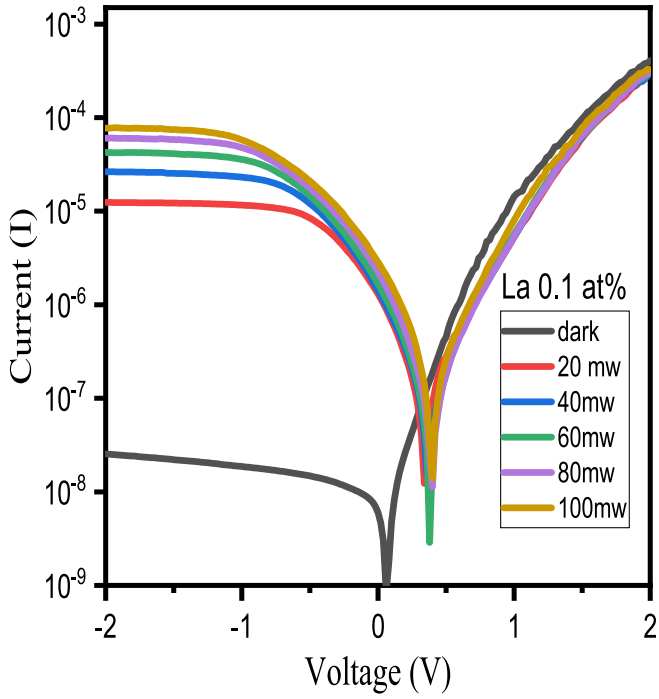

Fig. 5. The I-V plots of La (0.1 at%) and Zn (1 at%) co-doped CdO this film as photodetector.

$$I_s = AA^* exp\left(\frac{q(\varnothing_b)}{kT}\right) \tag{4}$$

where A^*, A, V,T,K, q, ϕ_b, and η in above equations are Richardson's constant (for p-type Si = 32 A/Cm^2 K^2), diode area, Voltage, Boltzmann constant, electron charge, potential barrier, and ideality factor, respectively. The observations of the *Al/p-Si/ La (0.1 at%)-Zn (1 at%)/ CdO/Al* photodetector and other results are reported in Table 1. The minimum ideality factor has been found to have a value of 1.8 by using equation (5), and the barrier height was obtained by rearranging equation (4), and to be 0.529. The values for the ideality factor increased as the concentration of La doping increased as well. Due to the ideality factor's value being greater than unity, these calculations show that the diode isn't ideal.

$$\eta = \frac{q}{kT}\left(\frac{dV}{d(lnI)}\right) \tag{5}$$

Additionally, as illustrated in Table 1, the ideality factor's high value indicates the existence of Inhomogeneities at the Schottky barrier, series

Table 1
Saturation current, barrier height, Ideality factor, and m values under illumination of light.

Illumination	Concentration at%	I_s (Ampere) Zn-La	$Ø_b$ (eV)($Φ_b$)	(*n*)	m value	Maximum Photoresponse
Solar light	Zn 1(alone)	6.12E-5	0.51	2.36	1.01	3796
Solar light	0.5 La (alone)	4.32E-5	0.5	3.2	0.97	2186
Solar light	0.1 Ln −Zn 1	2.86E-5	0.529	1.8	1.08	4085
Solar light	0.5 Ln −Zn 1	2.32E-5	0.534	2.1	1.16	
Solar light	2 Ln −Zn 1	2.41E-4	0.475	2.3	1.12	
Solar light	4 Ln −Zn 1	1.64E-4	0.486	2.6	1.06	

resistance, and interface states emanating from the layer of silicon oxide [33].

In order to better comprehend the photoresponse investigation of the photodetector, the transient photocurrent measures of the device were done using the different light intensities in Fig. 6.a. The photocurrent of the photodetector immediately reached a particular point when exposed to solar light irradiation at intensities that varied (20, 40, 60, 80, and 100 mW/cm2) and then gradually increased to the highest value. The photocurrent then returned to its initial state after shutting off. The Al/p-Si/La (0.1 at%)-Zn (1 at%)/CdO/Al photodetector's current I_{on}/I_{off} ratio was calculated to be about 4085 at 4.5 sec at 100 mW. Ameen et al. [21] found that the maximum photoresponse of the Cd-ZnO/p-Si photodetector was about 1400, and Soylu et al. [34] fabricated the device with a $GaFeO_3$ interlayer, and the photoresponse was about 15.

This indicates that the device behaves in a highly photoresponse manner [35] and significantly better than earlier works [1,36–38]. In addition, when the producing device's transient photocurrent measurements were evaluated, the rise and fall times had been determined. The response time is the time required for the photocurrent to increase from 10 % to 90 % of its maximum value. In the same way, the recovery time is similarly described (from 90 to 10 %). At 10 % of I_{off} and 90 % of I_{on}, the rise and recovery time for the first peak in Fig. 6a were measured to be 0.58 and 0.47 s, respectively.

Curves of capacitance versus time (C-t) of an *Al/p-Si/ La (0.1 at%)-Zn (1 at%)/ CdO/Al* photodetector measured at 10 kHz frequency and varied light intensities are demonstrated by Fig. 6. (b). It was found that photocapacitance improved as the intensity of the illumination increased, as illustrated in Fig. 6. (b). This indicates that the devices display photo conducting and photo capacitive behaviour and can be employed as optoelectronic phototransistor and photodetectors. An important use in optoelectronics is the rapidly changing optical signal, which is determined by a photodetector's response time to light illumination [39].

Furthermore, for all photodetector measurements of the photoresponse that changes with the various power intensities are displayed within Fig. 7 (a) The photodetector of *Al/p-Si/ La (0.1 at%)-Zn (1 at%)/ CdO/Al* exhibits a more effective photoresponse in comparison to the other concentration, as shown in Fig. 7a. The photodetector exhibits photoresponse behaviours together with high photocurrent values, low open circuit voltage, and low short circuit current. The photocurrent characterisation approaches that comparatively account for non-unity ideality components may be explored in the instance of interface states.

For the purpose of describing the photosensitivity of heterojunction photodetectors, photocurrent was plotted vs. the intensity of light illumination. Results from the (I_{ph} − P) plot can be seen in Fig. 7. (b) using Eq. (6) [34].

$$I_{Ph} = \alpha P^m \tag{6}$$

where, P represents the light illumination intensity and α represents a constant.

The graph shows that the photocurrent grew as light illumination intensity increased, and it also notes the linear relationship between the photocurrent and light intensity [40]. The determined m value was found to be greater than one (see Table 1). The ln (I_{ph}) vs. ln(P) graph illustrates that the aforementioned localized states' illumination coefficients below 100 mW/cm^2 are fitfully positioned in the mobility gap as due to the m value being greater than one [38,41]. The generated photodiode is expected to show a sub-linear photo-conductive behavior as a result of examining the *m* values discovered.

3.5. Capacitance-voltage, conductance-voltage, and interface state characteristics

Fig. 8 (a, b) show the C-V and G-V properties evaluated at ambient temperature as an expression of voltage and frequency for the *Al/p-Si/ La (0.1 at%)-Zn (1 at%)/ CdO/Al* photodetector device. Investigations of capacitance as well as conductance have been taken at the accumulation zone (−2 V) to the strong reversal region (2 V). C and G values dropped with increased frequency, as seen in Fig. 8 (a, b). The manufactured device's behavior differs from the ideal due to the existence of interface state in the *Al/p-Si/ La (0.1 at%)-Zn (1 at%)/ CdO/Al* photodetector.

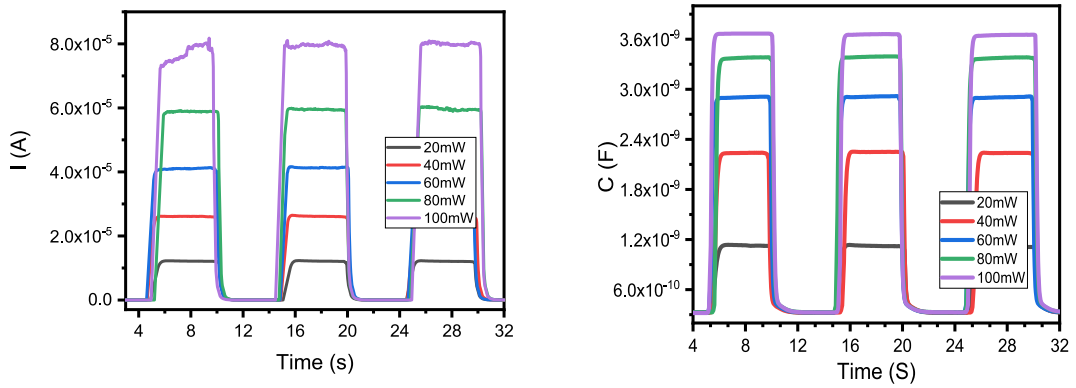

Fig. 6. (a) Photocurrent, and (b) Photocapacitance transient of La (0.1 at%) and Zn (1 at%) co-doped CdO film as photodetector.

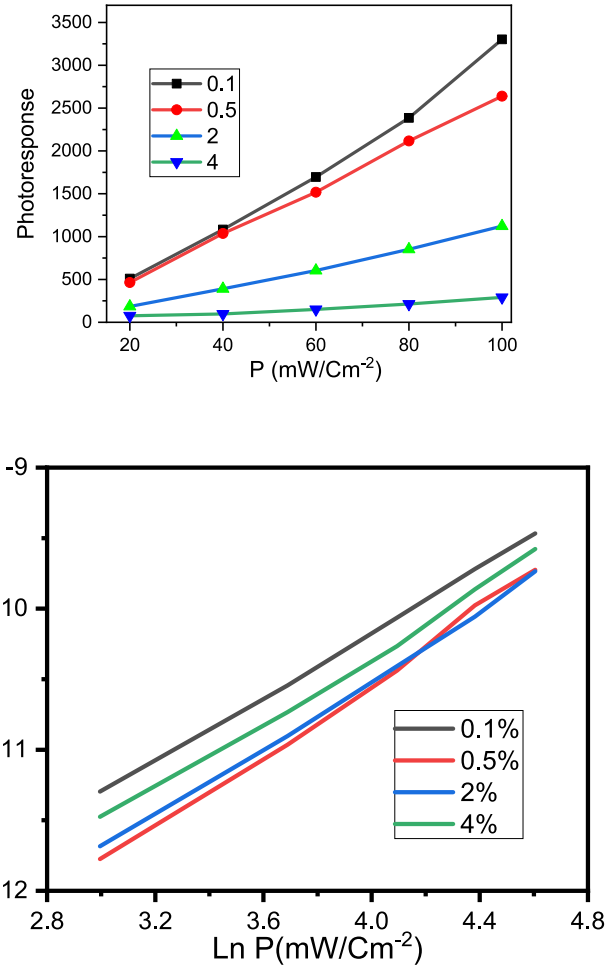

-b-

Fig. 7. (a) the photoresponse vs. power, (b) the Ln I_{ph} vs. Ln P Plot of the (different La and Zn1) at% co-doped CdO photodetector.

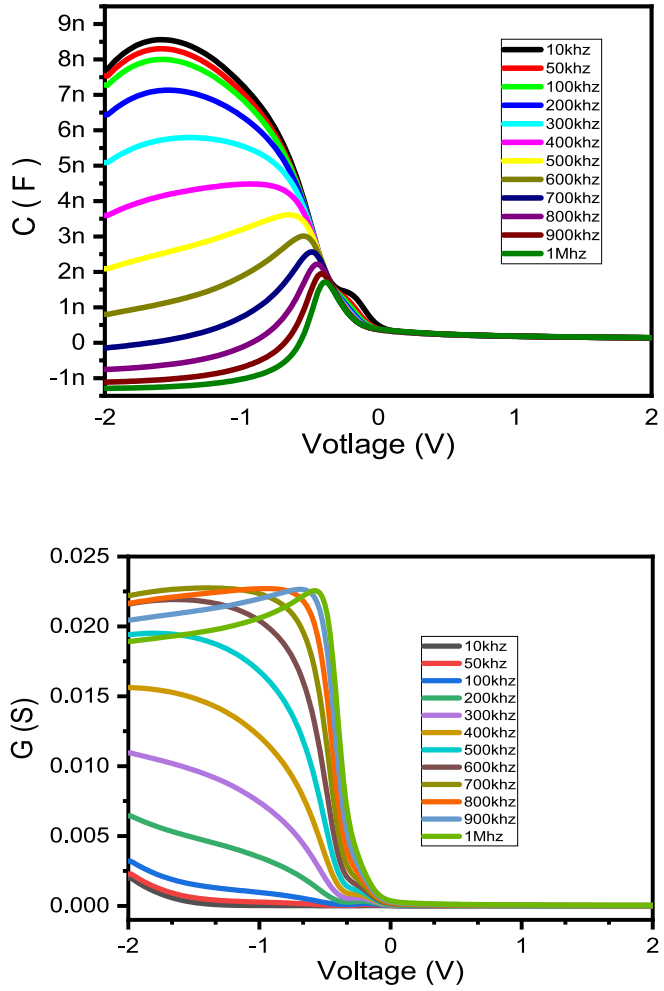

Fig. 8. A) c-v and b) g-v curves of the la (0.1 at%) and (zn1 at%) co-doped cdo photodetector.

Since the traps began to respond to the AC-signal, the values of the capacitance of the device grow with decreasing frequency. While the capacitance values decreased with increasing frequency, the conductance values increased. Interface states and series resistances have been correlated to this behavior of capacitance and conductance properties.

Such C/G-V curve behavior shows that there exist numerous interface state densities in the interface between deposited films and semiconductors, each of which has a varied life-time. Charging within the interface states cannot contribute to the capacitance of a properly constructed photodetector if capacitance measurements are performed at sufficiently high frequencies. This condition occurs once the time constant has been sufficiently long to enable the charge to respond both within and outside the interface states density in response to an applied signal [42,43].

Interface states and series resistances are critical concepts for diodes since they are the primary causes of non-ideal behaviour in diodes. The C-V as well as G-V values for all bias voltages and frequencies were adjusted by taking into account series resistance impacts. As a result, the true capacitance and conductance values of the *Al/p-Si/ La (0.1 at%)-Zn (1 at%)/ CdO/Al* photodetector were determined by Equations (7) and (8) [38,44].

$$C_{adj} = C_m \frac{(G_m^2 + (wC_m)^2)}{a^2 + (wC_m)^2} \tag{7}$$

$$G_{adj} = \frac{a(G_m^2 + (wC_m)^2)}{a^2 + (wC_m)^2} \tag{8}$$

Where $a = G_m - [G_m^2 + (wC_m)^2]R_s$, while R_s is the series resistance and the G_m and C_m terms were derived using an impedance analyser, G_{adj}, and C_{adj} are corrected conductance, and capacitance, respectively.

The C_{adj}-V and G_{adj}-V graphs' varied frequency effects are depicted in Fig. 9 (a, b). It is evident from this figure that the C_{adj} and G_{adj} vary with increasing frequency in the voltage of reverse bias; however, both were constant in the forward bias.

Fig. 9(b) demonstrates a peak at a reverse bias voltage's G_{adj} vs. voltage analysis. It has been shown that the peak intensity boosts with frequency, from 10 to 1000 kHz. The peaks existence in figures. 9 (a, b) are due to the series resistance [45]. To comprehend the nonlinear behavior exhibited by the corrected conductance and capacitance features, it is necessary to calculate the series resistance properties of the manufactured photodetector using the equations provided below [45,46].

$$R_s = \frac{G_m}{G_m^2 + (wC_m)^2} \tag{9}$$

As shown in Fig. 10 the series resistance value decreases with increasing frequency and the peaks like disappear at sufficient high frequencies. The results of the investigation can be understood by the existence of localized interface states. The trap charges have sufficient energy to

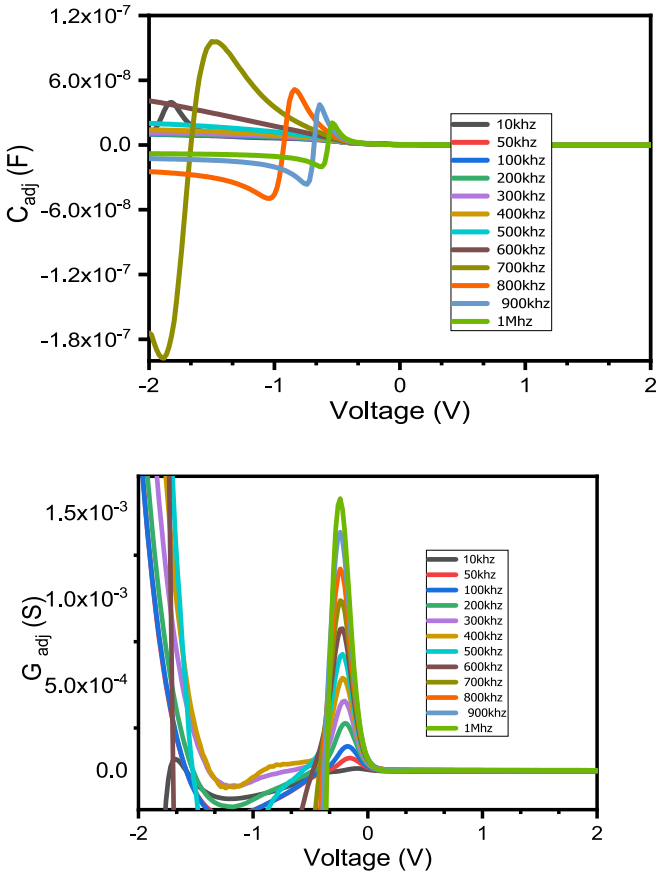

Fig. 9. A) the corrected c-v and b) the corrected g-v plot of the la (0.1 at%) and zn (1 at%) co-doped cdo photodetector.

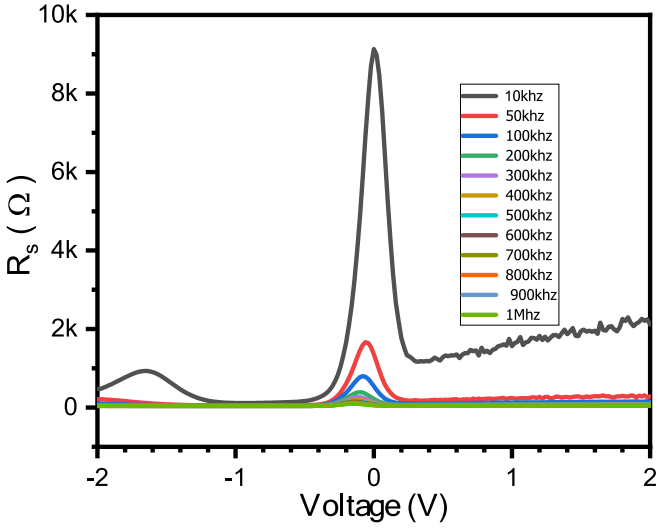

Fig. 10. The R_s-V plot of the La 0.1%-Zn1% co-doped CdO photodetector.

escape away from the traps situated at the metal–semiconductor interface, which might be the cause of these actions. Furthermore, at high frequencies, the interface states charge was unable to follow the alternate current signal.

In light of this data, the Hill-Coleman formula can be used to calculate the diode's interface state density (D_{it}) [47];

$$D_{it} = \frac{2(G_{adj}/w)_{max}}{q[(G_{max}/wC_{ox})^2 + (1 - C_m/C_{ox})^2]A} \quad (10)$$

herein, C_{ox} is stand for interlayer capacitance. The interface state density values for the manufactured photodetector have been calculated and the results were shown as a D_{it} versus V plot in Fig. 11. the value of the D_{it} has been determined to be around (2.3×10^{11} eV-1 cm^{-2}). As seen in Fig. 11 the D_{it} values declined exponentially with frequency, reaching roughly constant values at higher frequencies. In such a situation, the photodetector's capacitance increases due to the D_{it} at low frequencies extensively depend on frequency.

These observed behaviours are caused by interface states that exhibit weak reactions at high frequencies. One of the primary variables contributing to non-ideal photodetector results is the high D_{it} magnitude, which also affects significant parameters derived from I to V and C-V characteristics.

The observed enhancement in photoresponse with La-Zn co-doping is due to this doping creates a new energy level associated with the La-Zn exchange interaction with boosting extends electron-hole relaxation time, and creates a new energy level that significantly enhances charge transfer and light absorption thus, offers a promising mechanism for charge transfer and visible light harvesting [48].

4. Conclusion

In the present research, Al/p-Si/La-Zn co-doped CdO/Al photodetectors were fabricated by preparing CdO material with varying concentrations of La- and constant Zn co-dopant using sol–gel technology and spin depositing it onto a silicon substrate. The photoelectrical characteristics of the manufactured photodetector have been determined using measurements of current/capacitance–voltage and photo-transient. This measurement including the ideality factor, barrier height, and other crucial electrical characteristics such as photoconducting mechanism under solar light illumination. These results also revealed photoconductive and photocapacitive characteristics due to photocurrent of transient measurement. A further effect of the electrical properties is that voltage and frequency play a significant role in the established device's performance. To determine the transmission rate and energy band gap of the prepared films, optical measurements were performed. The device's current I_{on}/I_{off} ratio has been estimated to be approximately 4085 by the (La 0.1 and Zn 1) at% co-doping CdO, which indicates that it exhibits strong photoresponse behavior. The photodetector interface states that caused the deviation from ideality have been determined by calculations of C_{adj}-V and G_{adj}-V. The photodetector having La 0.1 and Zn 1) at% dopant exhibited that the highest photosensitivity of 6.3 $x10^{-4}$. The obtained results demonstrate that the optoelectronic achievement of metal/semiconductor devices using CdO is

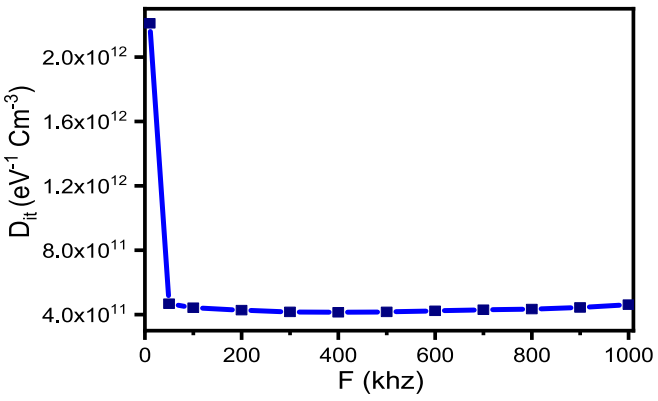

Fig. 11. The interface state density plot of the La (0.1 at%) and Zn (1 at%) co-doped CdO photodetector.

increased when La and Zn are included in the control at%. The results obtained demonstrate the applicability of the manufactured La-Zn co-doped CdO material in the technology of photovoltaic devices, particularly in photodiode applications. The produced (La 0.1 and Zn 1) at% co-doping CdO material is appropriate for solar device technology, particularly within photodetector applications, according to the outcomes of this study.

CRediT authorship contribution statement

Bestoon Anwer Gozeh: Writing – review & editing, Writing – original draft, Project administration, Methodology, Investigation, Formal analysis, Data curation, Conceptualization. **Lary H. Slewa:** Writing – review & editing, Writing – original draft, Software. **Cheman Baker Ismael:** Writing – review & editing, Writing – original draft, Visualization, Methodology, Investigation, Data curation, Conceptualization. **Sarwar Ibrahim Saleh:** Writing – review & editing, Writing – original draft, Visualization, Methodology, Formal analysis, Data curation. **Abdulkadir Yildiz:** Writing – review & editing, Writing – original draft, Visualization, Supervision. **Fahrettin Yakuphanoglu:** Writing – review & editing, Writing – original draft.

Funding

No funding was received for this work.

Declaration of competing interest

The authors declare that they have no known competing financial interests or personal relationships that could have appeared to influence the work reported in this paper.

Acknowledgments

Not applicable. Only authors mentioned in the author list contributed to this paper. There is no funding to acknowledge.

Authorship Contribution

Conception or design of the work (Dr. *Bestoon*).
Data collection (Dr. *Bestoon*).
Data analysis and interpretation (Dr. *Bestoon, Dr. Lary,*).
Drafting the article (*Bestoon, Dr. Lary*).
Critical revision of the article (Dr. *Bestoon, Dr. Lary, Dr. Cheman, Dr. Sarwar, Dr. Abdulkadir, Dr. Fahrettin*).
Final approval of the version to be published (Dr. *Bestoon, Dr. Lary, Dr. Cheman, Dr. Sarwar, Dr. Abdulkadir, Dr. Fahrettin*)

Data availability

Data will be made available on request.

References

[1] Vargas LMB, et al. Fast and broadband photoresponse in CdO thin film. J Lumin 2023;260:119873.
[2] Zamani M, Jamali-Sheini F, Cheraghizade M. Space-charge-limited current passivation of the self-powered and ultraviolet-to-visible range bilayer p-Si/n-Bi2S3 heterojunction photodetector by Ag coating. J Alloy Compd 2023;933:167665.
[3] Baghbanzadeh-Dezfuli B, Jamali-Sheini F, Cheraghizade M. Optoelectronic properties of nanostructured Sb2Se3 films synthesized by electrodeposition method: Effect of Zn concentrations. Sens Actuators, A 2022;344:113750.
[4] Cheraghizade M, Jamali-Sheini F. Space-charge-limited current activation in self-powered and solar-range nanostructured Cu3Se2 photodetector by Zn concentrations. Opt Mater 2023;143:114236.
[5] Gozeh BA, Karabulut A, Yildiz A, et al. SILAR Controlled CdS Nanoparticles Sensitized CdO Diode Based Photodetectors. SILICON 2020;12:1673–81. https://doi.org/10.1007/s12633-019-00266-7.
[6] Sahu VK, Misra P, Ajimsha RS, Das AK, Singh B. Effect of growth temperature on diode parameters of n-ZnO/p-Si heterojuction diodes grown by atomic layer deposition. Mater Sci Semicond Process 2016;54:1–5. https://doi.org/10.1016/j.mssp.2016.06.006.
[7] Hwang JD, Yan WJ. Using aluminum-induced polycrystalline silicon to enhance ultraviolet to visible rejection ratio of ZnO/Si heterojunction photodetectors. Sol Energy Mater Sol Cells 2015;134:227–30. https://doi.org/10.1016/j.solmat.2014.12.001.
[8] Tong C, Yun JY, Chen YJ, Ji DX, Gan QQ, Anderson WA. Thermally diffused Al:ZnO thin films for broadband transparent conductor. ACS Appl Mater Interfaces 2016;8:3985–91. https://doi.org/10.1021/acsami.5b11285.
[9] Gupta RK, Ghosh K, Patel R, Kahol PK. Bandgap engineering of rare earth element doped nanostructured cadmium oxide thin film. Phys E Low Dimens Syst Nanostruct 2011;44:163–7. https://doi.org/10.1016/j.physe.2011.08.009.
[10] S.K. Singh, P. Hazra, S. Tripathi, P. Chakrabarti, Performance analysis of RF sputtered ZnO/Si heterojunction UV photodetectors with high photoresponsivity, Superlattices Microstruct. 91 (2016) 62e69, https://doi.org/ 10.1016/j.spmi.2015.12.036.
[11] Aybek AS, Baysal N, Zor M, Turan E, Kul M. J Alloy Compd 2011;509:2530–4. https://doi.org/10.1016/j.jallcom.2010.11.077.
[12] Singh T, Pandya DK, Singh R. Synthesis of cadmium oxide doped ZnO nanostructures using electrochemical deposition. J Alloy Compd 2011;16:5095–8. https://doi.org/10.1016/j.jallcom.2011.01.168.
[13] Look DC, Reynolds DC, Eason DB, Cantwell G. Characterization of homoepitaxial p-type ZnO grown by molecular beam epitaxy 81 2002;2002e2004. https://doi.org/10.1063/1.1504875.
[14] C.Y. Liu, Y.C. Liu, Photoluminescence of CdxZn1−xO films grown on sapphire substrate by PLD technique, J. Alloy. Compd. 482 (2009) 393–395, https://doi.org/10.1016/j.jallcom.2009.04.029.
[15] H. Karami, A. Aminifar, H. Tavallali, PVA-based sol–gel synthesis and characterization of CdO–ZnO nanocomposite, J. Clust. Sci. 1 (2010) 1–9, https://doi.org/ 10.1007/s10876-009-0277-y.
[16] T. Jia, W. Wang, F. Long, Z. Fu, H. Wang, Q. Zhang, Fabrication, characterization and photocatalytic activity of La-doped ZnO nanowires, J. Alloys Compd. 484 (2009) 410e415, https://doi.org/10.1016/j.jallcom.2009.04.153.
[17] Yu Yun, Ma Yang, WenyuXing SongshengTao, Yangyang Chen, Su Tang, Wei Yuan, Jian Wei, Xi Lin, Qian Niu, X.C. Xie, Wei Han, Observation of long phasecoherence length in epitaxial La-doped CdO thin films, Phys. Rev. B 96 (2017) 245310.
[18] Velusamy P, Ramesh Babu R, Ramamurthi K, Elangovan E, Viegas J. Effect of La doping on the structural, optical and electrical properties of spray pyrolytically deposited, CdO thin filmsJournal of. Alloys Compd 2017;708:804–12.
[19] Ortega G, Santana A. Morales, Optoelectronic properties of CdO/Si photodetectors. Solid State Electron 2000;44:1765–9. https://doi.org/10.1016/S0038-1101(00)00123-4.
[20] Kumar BR, Prasad KH, Kasirajan K, Karunakaran M, Ganesh V, Bitla Y, et al. Enhancing the properties of CdO thin films by co-doping with Mn and Fe for photodetector applications. Sens Actuators A Phys 2021;319:112544. https://doi.org/10.1016/j.sna.2021.112544.
[21] Gozeh BA, Karabulut A, Ameen MM, Yildiz A, Yakuphanoğlu F. Synthesis and characterization of La-DOPED ZnO (La: ZnO) films for photodetectors. Surf Rev Lett 2020;27(07):1950173.
[22] W.A. Ameen, B. A. H., Yildiz, A., Farooq, F. Yakuphanoglu, Solar Light Photodetectors Based on Nanocrystalline Zinc Oxide Cadmium Doped/p-Si Heterojunctions, Silicon 11 (2019) 563–571. doi:10.1016/j.jallcom.2015.12.070.
[23] W.C. Huang, T.C. Lin, C.T. Horng, Y.H. Li, The electrical characteristics of Ni/nGaSb Schottky diode, Mater. Sci. Semicond. Process. 16 (2013) 418e423, https://doi.org/10.1016/j.mssp.2012.08.011.
[24] Bulakhe RN, Shinde NM, Thorat RD, Nikam SS, Lokhande CD. Deposition of copper iodide thin films by chemical bath deposition (CBD) and successive ionic layer adsorption and reaction (SILAR) methods. Curr Appl Phys 2013;3:1661–7. https://doi.org/10.1016/j.cap.2013.05.014.
[25] A. Fakhri, D. Salehpour Kahi, Synthesis and characterization of MnS2/reduced graphene oxide nanohybrids for with photocatalytic and antibacterial activity, J. Photochem. Photobiol. B Biol. 166 (2017) 259–263, https://doi.org/10.1016/j.jphotobiol.2016.12.017.
[26] Escobar-Alarcón L, Arrieta A, Camps E, Muhl S, Rodil S, Vigueras-Santiago E. An alternative procedure for the determination of the optical band gap and thickness of amorphous carbon nitride thin films. Appl Surf Sci 2007;254:412–5. https://doi.org/10.1016/j.apsusc.2007.07.052.
[27] Lang J, Fang Y, Zhang Q, Wang J, Li T, Li X, et al. Synthesis, characterization and photoluminescence property of La-doped ZnO nanoparticles. Appl Phys A 2016;122:1–7.
[28] Singh G, Chauhan MS. Synthesis and characterization of nanostructured La3+-doped CdO for photocatalytic application. Chem Phys Lett 2023;830:140810.
[29] Guo XC, Hao NH, Guo DY, Wu ZP, An YH, Chu XL, et al. β-Ga2O3/p-Si heterojunction solar-blind ultraviolet photodetector with enhanced photoelectric responsivity. J Alloy Compd 2016;660:136–40.
[30] Wu Z, Jiao L, Wang X, Guo D, Li W, Li L, et al. A self-powered deep-ultraviolet photodetector based on an epitaxial Ga2 O3/Ga: ZnO heterojunction. J Mater Chem C 2017;5(34):8688–93.
[31] Yu J, Dong L, Peng B, Yuan L, Huang Y, Zhang L, et al. Self-powered photodetectors based on β-Ga2O3/4H–SiC heterojunction with ultrahigh current on/off ratio and fast response. J Alloy Compd 2020;821:153532.
[32] Aslan N, Başman N, Uzun O, Erkovan M, Yakuphanoğlu F. The effects of deposition potential on the optical, morphological and mechanical properties of DLC films

produced by electrochemical deposition technique at low. Biomater Sci 2019;37:166–72. https://doi.org/10.2478/msp-2019-0023.
[33] N. Tugluo ̆ glu,- H. Koralay, K.B. Akgül, Çavdar, Analysis of inhomogeneous device parameters using current–voltage characteristics of identically prepared lateral Schottky structures, Indian J. Phys. 90 (2016) 43-48.
[34] Soylu M, Cavas M, Al-Ghamdi AA, Gafer ZH, El-Tantawy F, Yakuphanoglu F. Photoelectrical characterization of a new generation diode having GaFeO3 interlayer. Sol Energy Mater Sol Cells 2014;124:180–5. https://doi.org/10.1016/j.solmat.2014.01.045.
[35] O. Cicek, H.U. Tecimer, S.O. Tan, H. Tecimer, Altindal, I. Uslu, Evaluation of electrical and photovoltaic behaviours as comparative of Au/n-GaAs (MS) diodes with and without pure and graphene (Gr)-doped polyvinyl alcohol (PVA) interfacial layer under dark and illuminated conditions, Compos. Part B Eng. 98 (2016) 260e268, https://doi.org/10.1016/j.compositesb.2016.05.042.
[36] Gozeh BA, Karabulut A, Ismael CB, Saleh SI, Yakuphanoglu F. Zn-doped CdO effects on the optical, electrical and photoresponse properties of heterojunctions-based photodiodes. J Alloy Compd 2021;872:159624.
[37] Gozeh BA, Karabulut A, Yildiz A, Yakuphanoglu F. Solar light responsive ZnO nanoparticles adjusted using Cd and La Co-dopant photodetector. J Alloy Compd 2018;732:16–24.
[38] Gozeh BA, Karabulut A, Yildiz A, Dere A, Arif B, Yakuphanoglu F. SILAR controlled CdS nanoparticles sensitized CdO diode based photodetectors. SILICON 2020;12:1673–81.
[39] Lee D-K, Ko H, Cho Y. Single Si submicron wire photodetector fabricated by simple wet etching process. Mater Lett 2015;160:562–5.
[40] Li Y, Guo Y, Li Y, Zhou X. Fabrication of Cd-Doped TiO2 nanorod arrays and photovoltaic property in perovskite solar cell. Electrochim Acta 2016;200:29–36. https://doi.org/10.1016/j.electacta.2016.03.091.
[41] S. Demirezen, H.G. Çetinkaya, M. Kara, F. Yakuphanoğlu, Ş. Altındal, Synthesis, electrical and photo-sensing characteristics of the Al/(PCBM/NiO: ZnO)/p-Si nanocomposite structures, Sens. Actuators A Phys. (2021), https://doi.org/10.1016/j.sna.2020.112449.
[42] A. Türüt, On current-voltage and capacitance-voltage characteristics of metal semiconductor contacts, Turk. J. Phys. 44 (2020) 302–347, https://doi.org/10.3906/fiz-2007-11.
[43] Singh R, Narula AK. Junction properties of aluminum/ polypyrrole (polypyrrole derivatives) Schottky diodes. Appl Phys Lett 1997;71:2845–7.
[44] Turut A, Karabulut A, Ejderha K, Bıyıklı N. Capacitanceeconductance characteristics of Au/Ti/Al 2 O 3/n -GaAs structures with very thin Al 2 O 3 interfacial layer. Mater Res Express 2015;2:46301. https://doi.org/10.1088/2053-1591/2/4/046301.
[45] Nicollian EH, Goetzberger A. Mos conductance technique for measuring surface state parameters. Appl Phys Lett 1965;7:216–9.
[46] İ. Dokme, Ş. Altındal, T. Tunc, İ. Uslu, Temperature dependent electrical and dielectric properties of Au/polyvinyl alcohol (Ni, Zn-doped)/n-Si Schottky diodes, Microelectron. Reliab. 50 (2010) 39-44.
[47] W.A. Hill, C.C. Coleman, A single-frequency approximation for interface-state density determination, Solid State Electron. 23 (1980) 987e993, https:// doi.org/10.1016/0038-1101(80)90064-7.
[48] Raj ILP, Valanarasu S, Ade R, Bitla Y, Mohanraj P, Ganesh V, et al. Enhancing the ultraviolet photosensing properties of nickel oxide thin films by Zn–La co-doping. Ceram Int 2022;48(4):5026–34.